

## Domain analysis of supervillin, an F-actin bundling plasma membrane protein with functional nuclear localization signals

Julia D. Wulfkuhle\*, Irina E. Donina†, Nicole H. Stark, Robert K. Pope§, Kersi N. Pestonjamas<sup>p</sup>, Maria L. Niswonger<sup>¶</sup> and Elizabeth J. Luna<sup>||</sup>

Department of Cell Biology, University of Massachusetts Medical School, 377 Plantation Street, Worcester, MA 01605, USA

\*Present address: Laboratory of Pathology, NCI, Bldg 10, Room 2A33, 10 Center Drive, MSC 1500, Bethesda, MD 20892, USA

†Present address: Department of Biology, Tufts University, Medford, MA 02155, USA

§Present address: Naval Research Laboratory, Code 7303, Bldg 1105, Room D408C, Stennis Space Center, MS 39529-5004, USA

¶Present address: Antigenics, L.L.C., 630 Fifth Ave., Suite 2170, New York, NY 10111, USA

||Author for correspondence (e-mail: elizabeth.luna@ummed.edu)

Accepted 30 April; published on WWW 10 June 1999

### SUMMARY

**A growing number of actin-associated membrane proteins have been implicated in motile processes, adhesive interactions, and signal transduction to the cell nucleus. We report here that supervillin, an F-actin binding protein originally isolated from bovine neutrophil plasma membranes, contains functional nuclear targeting signals and localizes at or near vinculin-containing focal adhesion plaques in COS7-2 and CV1 cells. Overexpression of full-length supervillin in these cells disrupts the integrity of focal adhesion plaques and results in increased levels of F-actin and vinculin. Localization studies of chimeric proteins containing supervillin sequences fused with the enhanced green fluorescent protein indicate that: (1) the amino terminus promotes F-actin binding, targeting to**

**focal adhesions, and limited nuclear localization; (2) the dominant nuclear targeting signal is in the center of the protein; and (3) the carboxy-terminal villin/gelsolin homology domain of supervillin does not, by itself, bind tightly to the actin cytoskeleton in vivo. Overexpression of chimeras containing both the amino-terminal F-actin binding site(s) and the dominant nuclear targeting signal results in the formation of large nuclear bundles containing F-actin, supervillin, and lamin. These results suggest that supervillin may contribute to cytoarchitecture in the nucleus, as well as at the plasma membrane.**

Key words: Membrane skeleton, Focal adhesion, Vinculin, Alpha-actinin, Lamin, EGFP

### INTRODUCTION

Membrane skeletons are networks of cytoskeletal and membrane proteins that constitute transmembrane linkages between the extracellular surface and the underlying cortical cytoskeleton. Such specialized structures stabilize and shape the plasma membrane, and regulate membrane-dependent processes, including adhesion and extension of cell surface projections (Luna and Hitt, 1992). In adherent cells, actin-associated membrane skeletons include those associated with integrins at focal adhesions and cadherin/catenin-containing complexes at adherens junctions (Ben-Ze'ev, 1997; Gumbiner, 1996; Weisberg et al., 1997). These membrane skeletons not only mediate cell attachment to substrata and to adjacent cells, respectively, but also regulate cell growth and survival (Ruoslahti and Reed, 1994). Loss of either cell-substrate or cell-cell adhesion, especially when coupled with entry into the cell cycle, is associated with the transformation of the normally stationary epithelial cell into a more motile phenotype. Membrane skeleton proteins associated with sites of adhesion participate in this process, both as mechanical organizers of cell structure and as signaling agents to nuclear

targets during cell growth and differentiation (Lelièvre and Bissell, 1998).

A number of membrane skeleton proteins have been implicated in the formation and/or stabilization of cell surface protrusions. These proteins include actin-membrane linkers, such as the transmembrane protein ponticulin (Shutt et al., 1995) and the ERM protein family, which includes ezrin, moesin, and radixin (Bretscher, 1999; Vaheri et al., 1997). The formation of cell surface extensions also is potentiated by proteins that promote actin assembly and bundling in the vicinity of the plasma membrane (Furukawa and Fechheimer, 1997). For example, up-regulation of cellular levels of an F-actin bundling protein, such as fascin (Yamashiro et al., 1998), drebrin (Shirao, 1995), fimbrin/plastin (Arpin et al., 1994), or villin (Franck et al., 1990; Friederich et al., 1989), causes dramatic and characteristic changes in cell morphology.

As part of our ongoing effort to characterize the compositions and functions of membrane skeletons in motile cells, we have recently described a 205 kDa actin-binding membrane protein that we named supervillin (Pestonjamas et al., 1997). Supervillin, previously called p205, was initially identified as a major 205 kDa F-actin binding polypeptide in

HeLa cervical carcinoma cells (Luna et al., 1997) and in bovine neutrophil plasma membranes (Pestonjamas et al., 1997). Supervillin binds tightly and specifically to the sides of actin filaments (Pestonjamas et al., 1995) in F-actin blot overlay assays (Luna, 1998) and co-isolates with highly-stabilized actin filaments as part of a 26S complex from neutrophil membranes (Pestonjamas et al., 1997). Supervillin and neutrophil F-actin also co-immunoprecipitate after solubilization with stringent concentrations of detergents and salt, indicating tight binding under endogenous conditions (Pestonjamas et al., 1997). Supervillin protein (Pestonjamas et al., 1997) and message (Pope et al., 1998) are especially abundant in certain carcinoma cell lines, including HeLa S3 cervical carcinoma, SW480 adenocarcinoma, and A549 lung carcinoma cells.

Using an antibody directed against a 19 residue supervillin peptide (pepA), we observed previously that signal from this region of supervillin exhibited an intracellular localization that changed as a function of cell density and adherence state (Pestonjamas et al., 1997). In fully confluent Madin-Darby bovine kidney (MDBK) cells, anti-pepA signal was found with F-actin and E-cadherin at sites of cell-cell contact. In subconfluent cells that lacked significant amounts of cell-cell contact, the pepA epitope was enriched in nuclear and cytoplasmic punctae, as well as along the plasma membrane. Upon EGTA-mediated cell dissociation, the signal became internalized with E-cadherin and F-actin as a component of adherens junctions 'rings' (Kartenbeck et al., 1991). These results suggested that supervillin might play a role in the recruitment of actin filaments to adherens junctions and possibly to other cellular compartments, including the nucleus. However, the restricted nature of the epitope recognized by the antibody and the prevalence of nuclear localization artifacts in the literature (Melan and Sluder, 1992) limited the conclusions that we could draw from these data.

Analyses of the deduced amino acid sequences of bovine (Pestonjamas et al., 1997) and human (Pope et al., 1998) supervillin suggest that they are bipartite proteins with distinct amino- and carboxy-terminal domains. The amino termini of these two supervillins are 79.2% identical to each other but contain no obvious similarities to other characterized proteins. The only recognized protein motifs are three (human) or four (bovine) consensus sequences for nuclear localization signals (NLSs). By contrast, the carboxy-terminal ~775 amino acids of the two supervillins are 95.1% identical to each other and contain numerous consecutive sequences with extensive similarity to proteins in the gelsolin family of actin-binding proteins, which cap, nucleate, and/or sever actin filaments (Schafer and Cooper, 1995; Weeds and Maciver, 1993). This protein family also includes villin, a microvillar protein that contains six segments homologous to those in gelsolin plus a carboxy-terminal actin-binding 'headpiece' that confers actin filament bundling activity (Bazari et al., 1988; Bretscher, 1991; Finidori et al., 1992; Glenney et al., 1981). Although supervillin exhibits little or no similarity with the sequences in gelsolin/villin segment 1 that are required for actin filament severing (Way et al., 1989), ~50% sequence identity is observed between supervillin sequences (Pestonjamas et al., 1997) and regions in segment 2, segment 5, and the villin headpiece, all of which contain sites for binding F-actin (Weeds and Maciver, 1993). Thus, sequence analysis predicts

that the carboxy terminus of supervillin contains as many as three F-actin binding sites and suggests that the carboxy-terminal villin/gelsolin homology domain in supervillin may contain actin filament bundling and/or capping activities analogous to those of other members of this protein family (Schafer and Cooper, 1995).

To explore the intracellular localizations and functions of supervillin and to identify functional domains *in vivo*, we have expressed chimeras of supervillin sequences fused with the enhanced green fluorescent protein (EGFP; Cormack et al., 1996) in COS7-2 and CV-1 cells. In addition to the previously described localizations at the plasma membrane and in the nucleus, we find that full-length supervillin is concentrated at or near focal adhesion sites and can bind along stress fibers. Cells expressing high levels of supervillin exhibit dramatic changes in the architecture of the actin cytoskeleton, with a loss of focal adhesions and an increase in the numbers of cell protrusions and in the amounts of cytoplasmic F-actin and vinculin. Contrary to expectations raised by the similarity of the supervillin carboxy terminus to villin and gelsolin, our *in vivo* domain analyses suggest that the amino terminus of supervillin contains the major sites that promote F-actin bundling and targeting of supervillin to focal adhesions and stress fibers. Chimeras containing the first three NLSs in bovine supervillin can localize to the nucleus, but the dominant NLS apparently resides in the center of the protein between amino acids 831 and 1009. These results confirm the previously reported dual localizations of supervillin sequences at the plasma membrane and in the nucleus and demonstrate that supervillin can affect, either directly or indirectly, the integrity of focal adhesion plaques.

## MATERIALS AND METHODS

### Constructs

A full-length cDNA encoding bovine supervillin from nucleotides -80 to 5420 was obtained by PCR amplification with three sets of gene specific primers encompassing unique restriction sites along the supervillin upstream noncoding and coding sequences. Madin-Darby bovine kidney cDNA (Pestonjamas et al., 1997) served as template and PCR products were obtained with the Expand High Fidelity PCR System (Boehringer-Mannheim, Indianapolis, IN) and the following sets of primers: 5'-CACAAAAGAAGTATCGATGCTCAGC-3' and 5'-TCTGGCTTCGATATCTTCCA-GGG-3' encompassing the *ClaI* to *EcoRV* sites; 5'-CCCTGGAAGATATCGAAGCCAGACC-3' and 5'-CTTGACCTCTGCCCGGGCATC-3' encompassing the *EcoRV* to *SmaI* sites; 5'-AAGGACGATGCCCGGGCAGAGG-3' and 5'-AAACATCCATTTTCCTGGTCCATCAGTATTG-3' encompassing the *SmaI* to the *XbaI* site in the downstream noncoding sequence. The PCR products were each gel-purified and subcloned into the pBluescript II SK- or KS- vector (Stratagene, La Jolla, CA). Clones from each PCR product were sequenced until one was identified that did not contain artifacts resulting in changes in the amino acid sequence. These individual clones were then subcloned into pBluescript II SK- (Stratagene) to generate a full-length supervillin cDNA clone. This full-length clone was modified at the 5'-end by the replacement of the *ClaI* site at -80 nt with a linker oligo containing a *KpnI* site and at the 3'-end by the insertion of a linker containing a *XbaI* site into the *NotI* site of the vector. These modifications allowed for simple transfer of the supervillin cDNA into the mammalian expression vector system.

Fusion constructs encoding full-length supervillin or various

protein fragments were generated by subcloning into the pEGFPC and/or pEGFPN series of mammalian expression vectors (Clontech, Palo Alto, CA). The resulting chimeric proteins contained enhanced green fluorescent protein (EGFP), a more highly fluorescent variant (Cormack et al., 1996) of wild-type GFP (Prasher et al., 1992), at their amino- or carboxy termini, respectively. The supervillin fragments used in this study were generated using unique restriction sites along the supervillin sequence. The SV 1-830 fragment encompassed the *KpnI-EcoRV* noncoding and coding sequences; the SV 1-1009 fragment: *KpnI-EcoRI* sequences; SV 1010-1792 fragment: *EcoRI-XbaI* sequences; SV 830-1792: *EcoRV-XbaI* sequences; and the SV 831-1009 fragment: *EcoRV-SmaI* sequences. All fusion constructs were sequenced to ensure the maintenance of the proper reading frame before being amplified and purified with the Qiagen Endotoxin-Free Maxi Prep Kit (Qiagen, Santa Clarita, CA).

### Cell culture, transfections, and EGFP visualization

CV-1 cells, a monkey kidney epithelial cell line, was purchased from the American Type Culture Collection (Rockville, MD). The cells were maintained in MEM-alpha (Gibco/BRL, Grand Island, NY) supplemented with 10% fetal bovine serum. COS7-2 cells were the generous gift of Dr Kathleen J. Green, Northwestern University Medical School (Kowalczyk et al., 1997). They were maintained in DME/high glucose (DME/HG; Gibco/BRL) supplemented with 10% fetal calf serum.

COS7-2 or CV-1 cells were transfected with various EGFP-SV fusion or control constructs using the LipoTaxi Mammalian Transfection Kit (Stratagene) according to the manufacturer's instructions. Briefly, cells were plated onto sterile coverslips in 35 mm dishes at  $0.5\text{--}0.8 \times 10^5$  cells/ml 12-18 hours prior to transfection. Complex formation solutions containing 6  $\mu\text{g}$  DNA for fusion constructs or 5  $\mu\text{g}$  DNA for control constructs and 18  $\mu\text{l}$  of Lipotaxi reagent in 300  $\mu\text{l}$  of serum-free DME/HG were incubated 45 minutes at room temperature and then diluted with 500  $\mu\text{l}$  serum-free medium just prior to transfection. Cells were washed once with serum-free DME/HG and the 800  $\mu\text{l}$  complex formation solution was added to the dish. After incubation at 37°C for approximately 6 hours, 1.2 ml DME/HG with 20% serum was added to the dish and placed at 37°C overnight. The medium was replaced with 2 ml of normal growth medium the following day, and the cells were incubated again at 37°C for 24-48 hours before processing.

Fluorescence visualization of EGFP in cells was carried out as follows: cells were briefly washed in phosphate-buffered saline (PBS; 138 mM NaCl, 2.7 mM KCl, 8.1 mM  $\text{Na}_2\text{HPO}_4$ , 1.2 mM  $\text{KH}_2\text{PO}_4$ , pH 7.0) and then fixed in 3.7% EM grade formaldehyde (Electron Microscopy Sciences, Gibbstown, NJ) for 10 minutes at room temperature. The coverslips were then washed three times in PBS and mounted on slides in PBS and sealed with rubber cement. Cells were observed on a Zeiss Axioskop fluorescence microscope or a Bio-Rad MRC 1024 laser scanning confocal microscope (Bio-Rad Laboratories, Hercules, CA) equipped with LaserSharp Version 3.2 software.

### Antibodies and immunofluorescence

Transfected cells that were counterstained with antibodies or fluorescent phalloidin were fixed and washed as described above and then permeabilized in 1% Triton X-100 in PBS for 1 minute, washed 3 times in PBS and blocked for 1-4 hours at 37°C in blocking solution (10% horse serum, 1% BSA, and 0.02% sodium azide in PBS). Coverslips were then incubated with primary antibodies overnight at 4°C. The various primary antibodies used in this study were diluted into blocking solution as follows: monoclonal anti-human vinculin (Sigma Chemical Co., St Louis, MO) 1:400; monoclonal anti-alpha-actinin (Sigma) 1:200; and a rabbit polyclonal antibody recognizing lamins A and C, a generous gift from Dr Anne Goldman, Northwestern University Medical School, 1:400. F-actin was stained with Alexa 594<sup>TM</sup>-phalloidin (Molecular Probes, Inc., Eugene, OR) at

a concentration of 1 unit per coverslip. The coverslips were washed 3 times in PBS and then incubated for approximately 1 hour at room temperature with either Alexa 594<sup>TM</sup>-conjugated goat anti-rabbit IgG or Alexa 594<sup>TM</sup>-conjugated goat anti-mouse IgG (Molecular Probes, Inc.) diluted 1:2500 in blocking solution. The coverslips were again washed 3 times in PBS and then mounted and observed as described above.

### Triton pre-extraction and latrunculin-A experiments

To determine if EGFP-supervillin chimeras associated with the cytoskeleton, transfected cells were pre-extracted with 0.1% or 0.5% Triton X-100 in a cytoskeleton stabilizing buffer (50 mM NaCl, 3 mM  $\text{MgCl}_2$ , 30 mM sucrose, 10 mM Pipes, pH 6.8) (Adams et al., 1996) for 5 minutes or 2.5 minutes, respectively, at 4°C prior to fixation and antibody staining as described above. Latrunculin A (Molecular Probes, Inc.) was suspended in cell culture grade DMSO (Sigma) and diluted to a concentration of 5  $\mu\text{M}$  in cell culture medium. The latrunculin A-containing medium was added to cells 24 hours post-transfection and incubated for 4 hours at 37°C followed by fixation and/or phalloidin staining as described above.

## RESULTS

### Supervillin interactions with the actin cytoskeleton in vivo

In cells expressing low levels of EGFP-tagged bovine supervillin, the fluorescence signal was concentrated at the cell periphery, as linear arrays throughout the cytoplasm, and as occasional concentrations in or near the cell nucleus (Fig. 1A). The cytoplasmic and membrane fluorescence co-localized extensively with that from Alexa<sup>TM</sup> 594-phalloidin (Fig. 1B,C), suggesting that EGFP-tagged supervillin associates with membrane-associated F-actin and stress fibers. The avidity of the association between supervillin and the actin cytoskeleton was relatively high since it persisted after pre-extraction of lipids and soluble proteins with 0.5% Triton X-100 (Fig. 1D,E,F). As was especially evident in pre-extracted cells (Fig. 1F), there was a higher relative concentration of supervillin at the ends of actin filament bundles, hinting at an additional or preferential localization of supervillin at focal adhesion sites, where stress fibers are anchored through integrins and associated proteins to extracellular matrix components (Burridge and Chrzanowska-Wodnicka, 1996; Dedhar and Hannigan, 1996).

By contrast, in cells expressing only EGFP plus amino acids encoded by the multiple cloning site in the pEGFPC1 vector, fluorescence was observed throughout the transfected cells, apparently in proportion to the volume accessible to small proteins. Nuclei were bright because the diameter of the 27 kDa EGFP was well below the exclusion limit of ~9 nm (40-60 kDa) for passive diffusion through the nuclear pore (Peters, 1986). EGFP fluorescence also was observed throughout the cytoplasm, where the lower level of signal correlated with the reduced path length through these flattened cells (Fig. 1G). A limited co-localization with actin stress fibers (Fig. 1H) was sometimes seen (Fig. 1I), but any interactions between these vector-encoded sequences and the cytoskeleton were weak because the EGFP signal was readily extracted with even low concentrations of detergent (Fig. 1J,K,L).

Cells expressing high levels of EGFP-tagged (Fig. 2A,D,G) or untagged (not shown) supervillin were distinguishable by

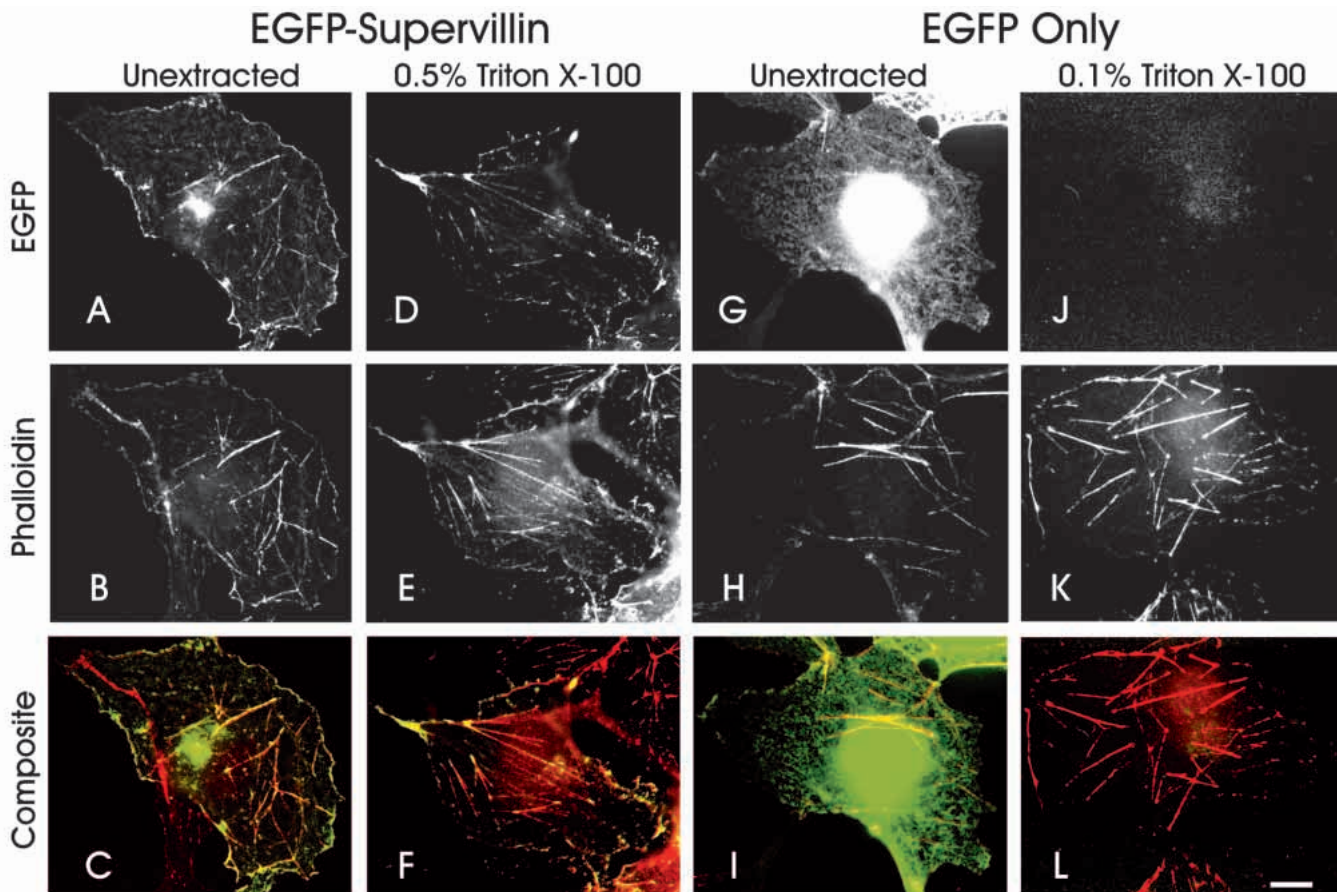


**Fig. 1.** Supervillin localizes preferentially to the plasma membrane and at actin filament bundles in COS7-2 cells. Co-localization of EGFP-tagged supervillin (A,D) and EGFP only (G,J) with Alexa<sup>TM</sup> 594-labeled phalloidin (B,E,H,K) in COS7-2 cells that were fixed before (A-C, G-I) or after extraction with 0.5% Triton X-100 (D-F) or after extraction with 0.1% Triton X-100 (J-L). Composite images (C,F,I,L) were generated by superimposition of the EGFP (green) and phalloidin (red) signals; areas of overlap appear yellow. Bar, 20  $\mu$ m.

their rounded morphologies, jagged borders, and numerous spiky projections. F-actin co-localized with the supervillin-induced projections (Fig. 2B,C,E,F) and was also increased in these cells, as judged by the enhanced amounts of phalloidin staining relative to that in surrounding untransfected cells (Fig. 2B,E). These high levels of supervillin and F-actin were retained after extraction with 0.5% Triton X-100, indicating association with the cytoskeleton. Vinculin, a component of the focal adhesion plaque (Burrige and Chrzanowska-Wodnicka, 1996; Craig and Johnson, 1996), also appeared to be up-regulated and re-distributed in cells expressing high levels of supervillin (Fig. 2G,H,I). This reorganization was caused by supervillin overexpression because no change in vinculin distribution was observed in cells overexpressing only EGFP (Fig. 2J,K,L). These results showed that increased levels of supervillin induce a major reorganization of the actin-based cytoskeleton *in vivo* and suggest that supervillin potentiates the formation of actin filament bundles.

#### Domain analysis of supervillin

To localize functional targeting and F-actin binding sequences within supervillin, we used conveniently-located unique restriction sites to generate chimeras between EGFP and bovine supervillin sequences (Fig. 3). We first tested the hypothesis that the carboxy-terminal villin/gelsolin homology

domain is responsible for the observed association of full-length supervillin with the actin cytoskeleton. An EGFP-tagged chimeric protein containing the entire villin/gelsolin homology domain of supervillin (EGFP-SV1010-1792), including all three predicted actin-binding sites (Fig. 3, AB Sites), was transiently transfected into COS7 and CV1 cells (Fig. 4). Surprisingly, EGFP-SV1010-1792 was diffusely distributed throughout the cytoplasm (Fig. 4A,G) with little or no obvious co-localization with actin filament bundles (Fig. 4B,C), even in CV1 cells which have extensive arrays of stress fibers (Fig. 4H,I). Also, 0.1% Triton X-100 released essentially all the EGFP-SV1010-1792 from both cell types (Fig. 4D,E,F,J,K,L), suggesting that the villin/gelsolin homology domain of supervillin, by itself, does not bundle actin filaments or bind F-actin with high affinity.

To test the hypothesis that the amino-terminal domain of supervillin contains functional nuclear localization signals (Fig. 3, NLSs), we transfected COS7 and CV1 cells with an EGFP-tagged chimeric protein containing the first 1009 residues of supervillin (EGFP-SV1-1009). In fact, EGFP-SV1-1009 (Fig. 5A, green) was targeted to cell nuclei (Fig. 5A, blue), where it formed large, looping coils visible even in phase optics (Fig. 5B). In addition, EGFP-SV1-1009 localized at cell borders, in membrane ruffles, and in linear cytoplasmic arrays (Fig. 5A,C), in association with phalloidin-stained actin

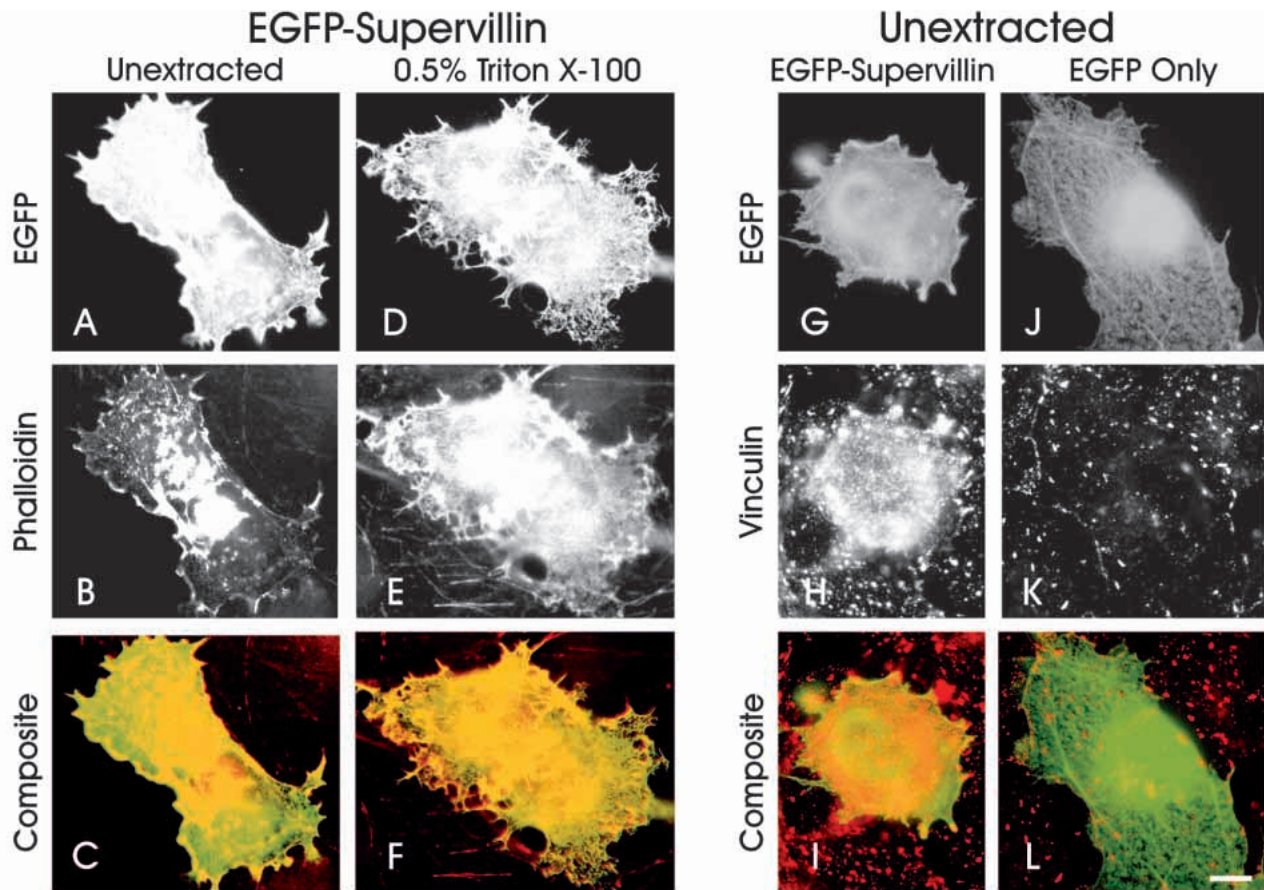
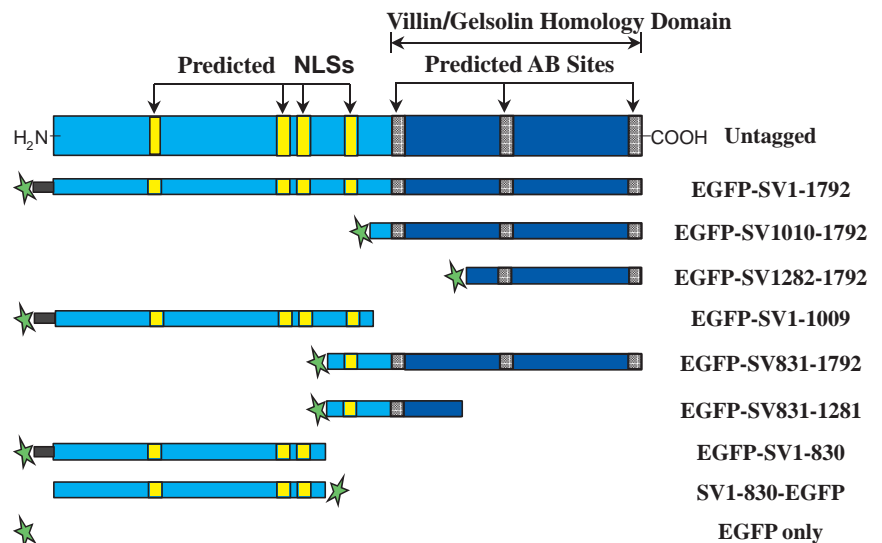


**Fig. 2.** Supervillin overexpression induces dramatic changes in cell morphology and in the actin cytoskeleton. COS7-2 cells expressing high levels of EGFP-tagged supervillin (A-I) or EGFP only (J-L) were fixed before (A-C, G-L) or after (D-F) extraction with 0.5% Triton X-100 and counter-staining with Alexa™ 594-phalloidin (B,C,E,F) or with antibodies against vinculin (H,I,K,L). Composite images (C,F,I,L) show the superimposition of the EGFP (green) and phalloidin (red) signals; areas of overlap appear yellow. The levels of total F-actin (B,C,E,F) and vinculin (H,I) are greatly increased in cells that overexpress EGFP-supervillin (A,D,G), as compared with the surrounding untransfected cells that are present in all these panels. Bar, 20 µm.

**Fig. 3.** Diagrammatic representations of the predicted domain structure of bovine supervillin and the structures and names of the chimeric proteins used in this study. Sequence analysis predicts that the amino terminus of supervillin contains four nuclear localization signals (NLSs) and that the carboxy terminus contains as many as three actin binding (AB) sites and other regions of sequence similarity with villin and gelsolin, beginning with the F-actin binding site in villin/gelsolin subdomain 2 (Pestonjams et al., 1997). The location of EGFP is indicated with a star; the small black bar denotes the presence of a 27 amino acid segment encoded by sequences in the supervillin 5'-UTR that are downstream of the cloning site and immediately upstream of the initiator methionine.



filaments (Fig. 5C, co-localization shown as yellow). The large nuclear coils containing EGFP-SV1-1009 also labeled intensely with Alexa™ 594-phalloidin (Fig. 5D,H). Both the

cytoplasmic filaments (not shown) and the nuclear coils (Fig. 5D) that were associated with EGFP-SV1-1009 resisted extraction with 0.5% Triton X-100, indicating that both of

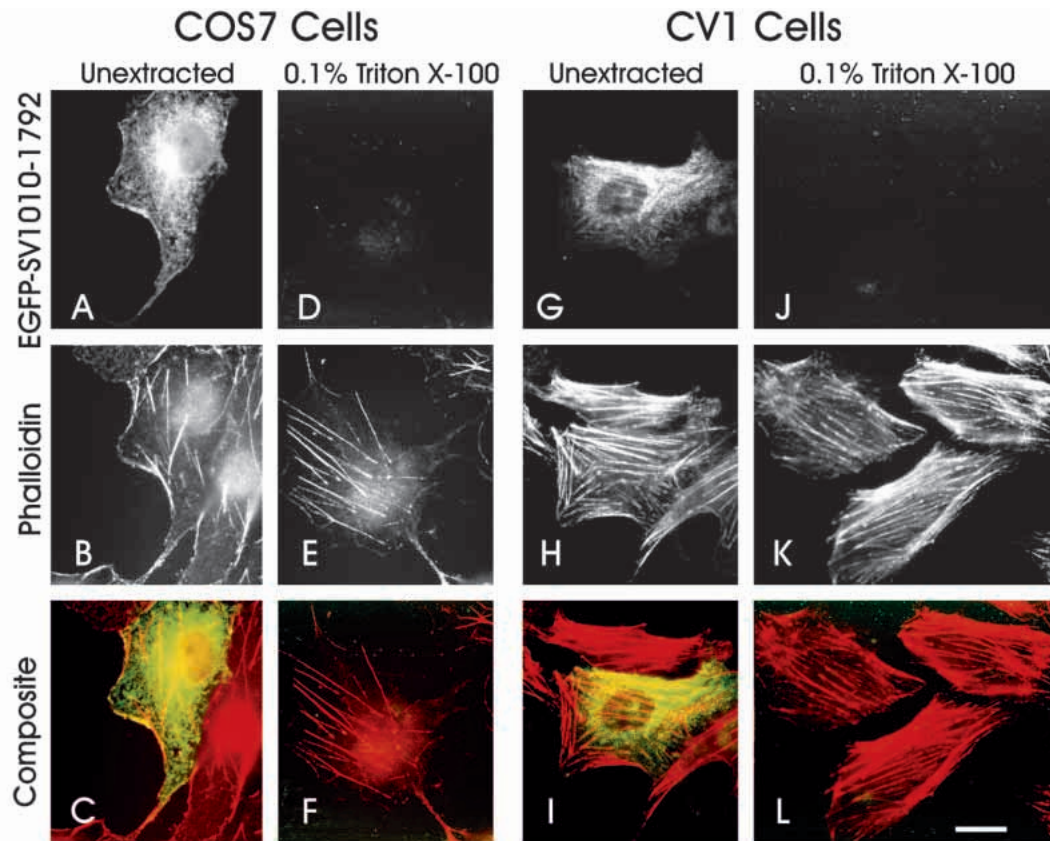


**Fig. 4.** The villin/gelsolin homology domain of supervillin is apparently not tightly associated with the actin cytoskeletons of COS7-2 (A-F) or CV1 (G-L) cells. Lack of co-localization of EGFP-SV1010-1792 (A,D) with Alexa<sup>TM</sup> 594-labeled phalloidin (B,E,H,K) in cells that were fixed before (A-C, G-I) or after extraction with 0.1% Triton X-100 (D-F, J-L). Composite images (C,F,I,L) show only a weak coincidence of labeling in cells that were fixed before permeabilization (C,I), and little EGFP-SV1010-1792 remains after detergent extraction (F,L). Bar, 20  $\mu$ m.

these structures contained bundled actin filaments. In general, the EGFP-SV1-1009 localization was either predominately nuclear or predominately cytoplasmic within a cell, but could vary widely between cells on the same coverslip. As a rule, nuclear coils were much more prevalent in the highly transformed COS7-2 cells, whereas the extensive system of stress fibers was more commonly labeled in the CV-1 cells.

The nuclear bundles of F-actin and EGFP-SV1-1009 appeared to have a composition distinct from that of cytoplasmic actin filaments. First, unlike cytoplasmic actin filaments (Fig. 5E), the F-actin/EGFP-SV1-1009 nuclear bundles contained essentially no associated alpha-actinin (Fig. 5F). Even cytoplasmic actin filaments that contained both EGFP-SV1-1009 and alpha-actinin exhibited little signal overlap; linear cytoplasmic arrays that appeared to stain for both proteins usually consisted of dashes of alternating red and green signal with few or no regions of yellow overlapping fluorescence (Fig. 5E). Second, F-actin/EGFP-SV1-1009 nuclear bundles also contained appreciable amounts of lamins A/C (Fig. 5G, red, overlap in yellow), intermediate filament proteins that are structural components of the nuclear envelope (Gant and Wilson, 1997; Moir et al., 1995). Finally, F-actin/EGFP-SV1-1009 nuclear bundles were distinguishable from cytoplasmic actin filaments in that they were stable after treatment of cells with latrunculin A, a marine toxin that disrupts the actin cytoskeleton by binding and sequestering

monomeric actin (reviewed by Ayscough, 1998). Even treatment with 5  $\mu$ M latrunculin A for four hours, a condition ten times more stringent than that required for the disruption of cytoplasmic actin filaments (Fig. 5H, red) did not destabilize the F-actin/EGFP-SV1-1009 nuclear bundles (Fig. 5H, co-localization in yellow), suggesting that these filament bundles are differentially stabilized against depolymerization. These results show that the amino-terminal domain of supervillin not only is capable of targeting supervillin to the nucleus, but also can recruit F-actin into the nucleus and can bundle actin filaments into a novel structure.

The dominant nuclear targeting signal in supervillin appeared to be located in the center of the molecule. Addition of supervillin residues 831-1009 to the villin/gelsolin homology domain in the EGFP-tagged carboxy-terminal chimeric protein, EGFP-SV831-1792, targeted the protein to the nucleus (Fig. 6A), where it was sequestered both as a diffuse nucleoplasmic distribution and as detergent-insoluble aggregates (Fig. 6B) that were visible in phase optics (Fig. 6A,B, insets). Limited co-localization of Alexa<sup>TM</sup> 594-phalloidin with the aggregated EGFP-SV831-1792 (Fig. 6A,B, green-yellow) hinted at a low incorporation of F-actin into these aggregates. Nuclear targeting, nuclear aggregation, detergent insolubility, and limited binding to Alexa<sup>TM</sup> 594-phalloidin also were observed for EGFP-tagged residues 831-1281 (Fig. 6C,D, EGFP-SV831-1281). No association with

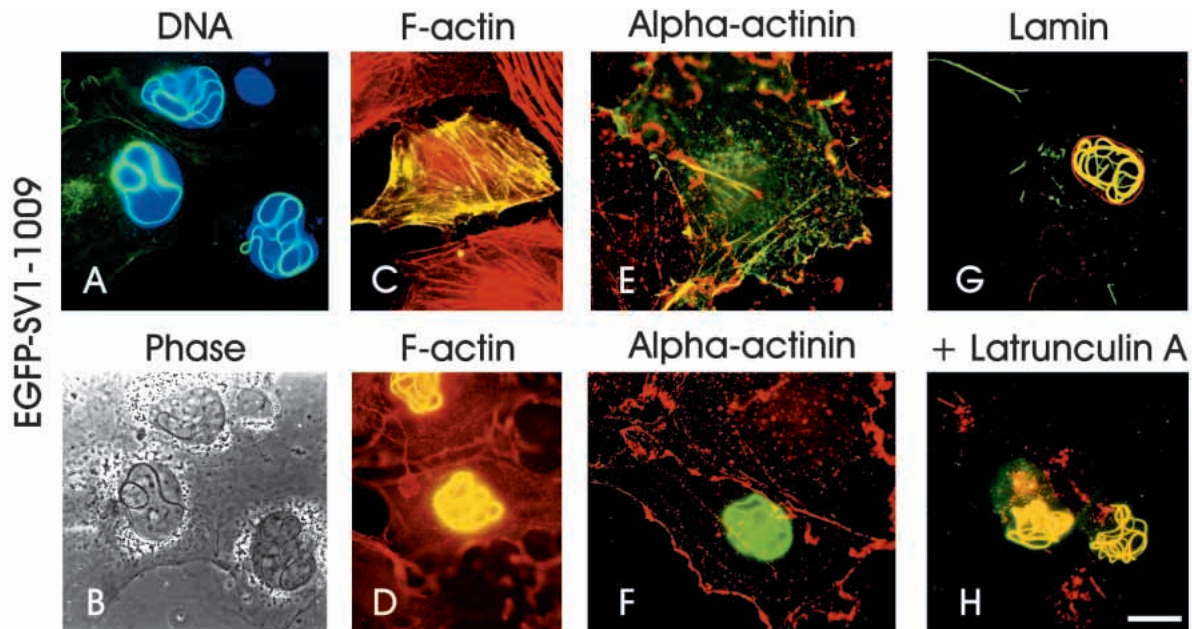


**Fig. 5.** EGFP-SV1-1009 exhibits two types of intracellular distributions in COS7-2 cells (A,B,D,E,F,G,H) and CV1 cells (C). Cytoplasmic signal is seen in association with the plasma membrane (A,E,G, green) and with F-actin containing stress fibers (C, yellow); nuclear EGFP-SV1-1009 appears as large looping coils visible with phase optics (B), as well as with fluorescein filters and epifluorescence (A,D,F,H) or confocal (G) microscopy. DNA was visualized with Hoechst dye (A, blue), F-actin with Alexa<sup>TM</sup> 594-phalloidin (C,D,H), and alpha-actinin (E,F) and lamins A/C (G) with specific antibodies and Alexa<sup>TM</sup> 594-labeled secondary antibodies. Some cells were pre-extracted with 0.5% Triton X-100 (D) or were pre-treated for 4 hours with 5  $\mu$ M latrunculin A (H) before fixation. In composite images (A, C-H), the EGFP-SV1-1009 fluorescence is shown in green, Hoechst dye in blue, and F-actin, alpha-actinin, and lamin in red; yellow represents overlap of green and red signals. Bar, 20  $\mu$ m.

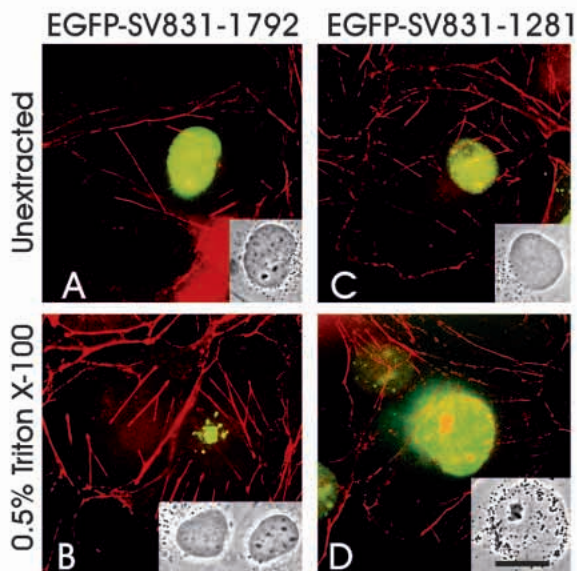


**Fig. 6.** EGFP-SV831-1792 (A, B) and EGFP-SV831-1281 (C, D) are targeted to the nuclei of transfected COS7-2 cells, where they form aggregates visible in phase (insets) that resist pre-extraction with 0.5% Triton X-100 (B, D). Composite images show EGFP fluorescence in green and the localization of F-actin stained with Alexa<sup>TM</sup> 594-phalloidin in red. Bar, 20  $\mu$ m.

cytoplasmic actin filaments (Fig. 6, red) or recruitment of actin into filament bundles was observed with either of these chimeric proteins.

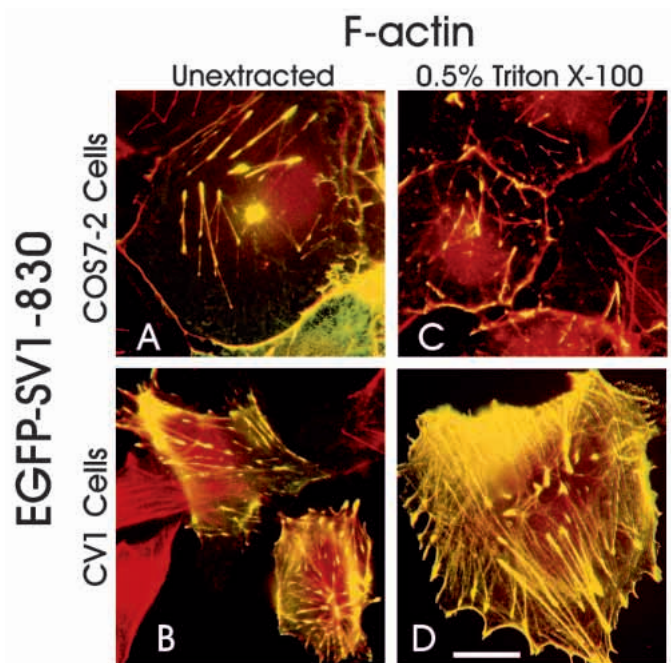
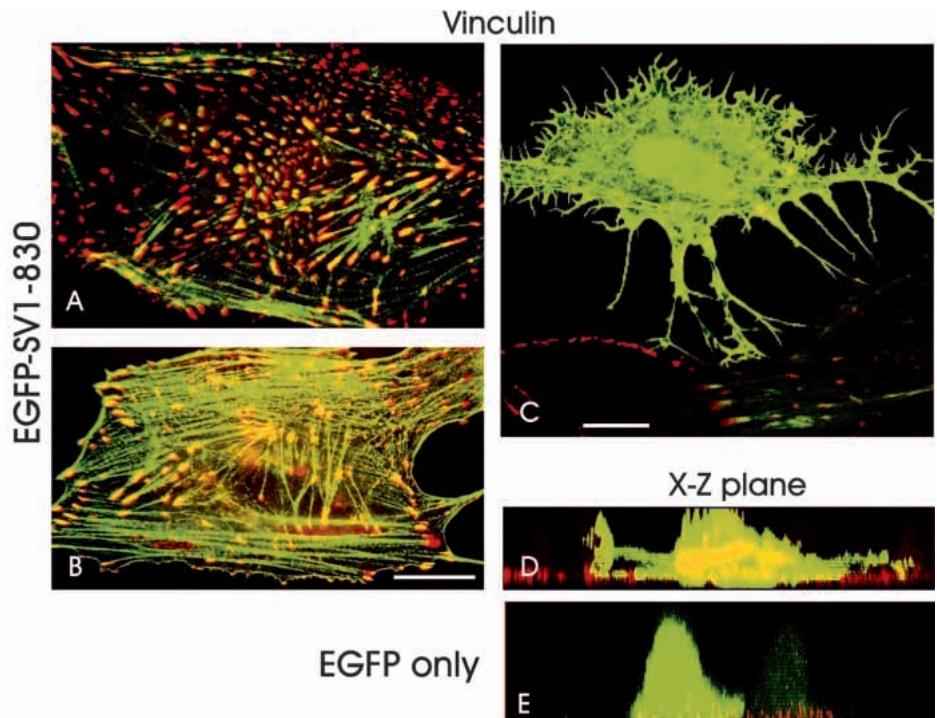


**Fig. 7.** EGFP-SV1-830 co-localizes extensively with F-actin at the plasma membrane, along stress fibers, and in 'arrowheads' at the ends of stress fibers. COS7-2 cells (A,C) and CV1 cells (B,D) expressing EGFP-SV1-830 (green) were fixed before (A,B) or after (C,D) extraction with 0.5% Triton X-100 and counter-staining with Alexa<sup>TM</sup> 594-phalloidin (red). Composite images show the superimposition of the two signals with areas of overlap appearing yellow. Bar, 20  $\mu$ m.

**Fig. 8.** At low (A) expression levels, the distribution of EGFP-SV1-830 overlaps that of vinculin at focal adhesion plaques. At moderate (B) expression levels, both focal adhesion and stress fiber staining is observed. High expression levels (C-D) cause changes in cell morphology and disruption of vinculin localization at ventral cell surfaces. CV1 cells expressing EGFP-SV1-830 (A-D) or EGFP vector sequences only (E) were counter-stained with anti-vinculin and Alexa™ 594-secondary antibody. Images were obtained with epifluorescence (A, B) or confocal (C-E) microscopy. Composite images show EGFP fluorescence in green, vinculin localization in red, and areas of overlap as yellow. Bars: 20 µm (A,B); 10 µm (C-E).



By contrast, the first 830 amino acids of supervillin were associated with cytoplasmic actin-containing structures (Fig. 7). Chimeric proteins containing EGFP at either the amino terminus (EGFP-SV1-830; Fig. 7) or carboxy terminus (SV1-830-EGFP, not shown) localized preferentially to the plasma membrane and along stress fibers and were especially highly concentrated at the ends of stress fibers in arrowhead-shaped structures. Binding interactions at all these sites were high enough to resist pre-extraction with 0.5% Triton X-100 (Fig. 7C,D). A small but consistent fraction of these transfected cells, ~5% for EGFP-SV1-830 and ~30% for SV1-830-EGFP, also exhibited nuclear actin bundles similar to those generated by EGFP-SV1-1009 (data not shown).

As was observed with full-length supervillin, EGFP-SV1-830 (Fig. 8, green) co-localized with vinculin (Fig. 8, red) at arrowhead-shaped focal adhesion plaques in cells expressing low levels of transfected protein (Fig. 8A,B). Although the overlap between the EGFP-SV1-830 and vinculin signals at focal adhesions was extensive (Fig. 8A,B, yellow), it was far from complete, indicating that not all vinculin-rich sites were associated with significant amounts of the tagged supervillin amino terminus. At high expression levels, EGFP-SV1-830 apparently disrupted the structure of the focal adhesion plaques and altered the cell morphology (Fig. 8C,D). Cells appeared less adherent to the substrate and exhibited many spike-like cell surface protrusions reminiscent of those observed in cells overexpressing full-length supervillin (Fig. 2). Confocal sections through the ventral surfaces of these cells showed only occasional regions of overlap between EGFP-SV1-830 and vinculin (Fig. 8C, yellow). Additionally, X-Z cross-sections of cells expressing high levels of EGFP-SV1-830 showed that the amount of vinculin was increased and its distribution was altered, with EGFP-SV1-830 and vinculin co-localizing in large bar-like cytoplasmic structures (Fig. 8D). For instance, note that the yellow signal (EGFP-SV1-830 + vinculin) in the center cell shown in Fig. 8D is both more intense and further

from the substratum than is the red signal (vinculin only) in the flanking, untransfected cells. Vinculin levels and localizations were unaffected by comparable overexpression of EGFP alone (Fig. 8E). Thus, most of the morphological effects observed in cells overexpressing full-length supervillin also are observed upon overexpression of amino acids 1 through 830.

## DISCUSSION

In agreement with previous biochemical and immunological observations (Pestonjamas et al., 1995, 1997), we show here that supervillin associates with actin filaments at the plasma membrane. In addition, we report that overproduction of supervillin induces dramatic changes in the architecture of the cortical actin-based cytoskeleton and apparently increases the amounts of cellular F-actin and vinculin. We further demonstrate that supervillin can potentiate actin filament bundling and the recruitment of actin into bundles at the plasma membrane and in the cell nucleus.

Additionally, we show that supervillin localizes at or near a subset of vinculin-containing focal adhesion plaques, a localization not observed in our previous study with MDBK cells and antibodies generated against a supervillin peptide. We have since found that EGFP-SV1-830 also localizes with vinculin-staining focal adhesion plaques in MDBK cells (data not shown), suggesting that the epitope(s) recognized by our anti-peptide antibody may not be accessible in focal adhesion plaques. A similar lack of accessibility has been observed with antibodies against alpha-actinin (Pavalko et al., 1995).

### Overexpression phenotype

In many respects, cells transfected with vectors encoding actin-bundling sequences in supervillin (Figs 2, 8) resemble cells that have been induced to overexpress, or have been microinjected with, other F-actin bundling proteins. For instance, long cell

surface extensions also are generated by overproduction of drebrin (Shirao et al., 1992) and 'spiky' cell borders are observed in cells overexpressing fascin (Yamashiro et al., 1998) and in some cells containing high intracellular levels of villin (Franck et al., 1990). Overproduction of T- or L-plastin induces cell rounding and a reorganization of stress fibers; both plastins also co-localize with vinculin at basal cell surfaces and decrease the numbers of focal adhesion sites (Arpin et al., 1994). Villin also can induce re-distribution of vinculin from focal adhesions into a diffuse cytoplasmic 'cloud' (Franck et al., 1990) that is reminiscent of the cytoplasmic vinculin localization in cells expressing high levels of supervillin. However, whereas villin overexpression leads to a disappearance of actin from stress fibers, apparently due to the recruitment of actin into core bundles inside elongating microvilli (Franck et al., 1990; Friederich et al., 1989), supervillin, like drebrin (Ikeda et al., 1996; Shirao et al., 1992), increases cellular concentrations of both F-actin and vinculin. Increased levels of F-actin and vinculin also are observed in cells treated with phalloidin (Bershadsky et al., 1995), a drug that blocks monomer dissociation from actin filaments (Coluccio and Tilney, 1984). Thus, a number of actin bundling proteins, including supervillin, may increase total cellular F-actin by inhibiting actin depolymerization.

The disruption of focal adhesion plaque structure by supervillin may correlate with the observation that the intracellular localizations of supervillin and alpha-actinin appear to be mutually exclusive. The actin bundling and membrane association activities of alpha-actinin-1 are important for stress fiber integrity, for the formation and extent of focal adhesion plaques, and for the adhesion of cells to each other and to the substrate (Glück and Ben-Ze'ev, 1994; Glück et al., 1993; Knudsen et al., 1995; Pavalko and Burridge, 1991; Schultheiss et al., 1992). While two or more actin bundling proteins apparently cooperate to form actin filament bundles in intestinal brush border microvilli (reviewed by Bretscher, 1991; Fath and Burgess, 1995; Heintzelman and Mooseker, 1992; Louvard et al., 1992), *Drosophila* neurosensory bristles (Tilney et al., 1995; Wulfschuh et al., 1998), stereocilia (reviewed by Tilney et al., 1992), and *Drosophila* nurse cell ring canals (reviewed by Robinson and Cooley, 1997), non-synergistic pairs of actin bundling proteins also are known. For instance, drebrin interferes with the actin binding and bundling activities of both alpha-actinin (Ishikawa et al., 1994) and fascin (Sasaki et al., 1996). Thus, actin filaments bundled by supervillin may have different spacings or crosslink periodicities than do F-actin bundles enriched in alpha-actinin (Taylor and Taylor, 1994). This could lead to a dichotomy of F-actin bundles in supervillin-overexpressing cells and to decreased numbers of stress fibers anchored at focal adhesions through alpha-actinin and associated proteins. Alternatively, supervillin may disrupt focal adhesion plaque integrity by directly interfering with the functioning of another essential component of the plaque.

### Supervillin functional domains

Our results suggest a new model for supervillin functional domains (Table 1, Fig. 9). In this model, the primary membrane and cytoskeleton targeting sites are in the amino terminus, the dominant nuclear targeting signal is in the center of the polypeptide, and the villin/gelsolin homology domain with its still largely undetermined function is at the carboxy terminus.

**Table 1. Triton insolubility and intracellular localizations of the constructs employed in this study**

Construct	Triton insolubility	Intracellular localization(s)
EGFP-SV1-1792	++	PM, SF, nucleus
SV1-1792	n.d.	PM, SF, nucleus
EGFP-SV1-830	++	SF, FA, PM
SV1-830-EGFP	++	SF, FA, PM, nucleus
EGFP-SV1-1009	+++	Nucleus, PM, SF, FA, agg
EGFP-SV831-1792	+	Nucleus, agg
EGFP-SV831-1281	+	Nucleus, agg
EGFP-SV1010-1792	-	Cytoplasm, nucleus
EGFP-SV1282-1792	-	Cytoplasm, nucleus
EGFP only	-	Nucleus, cytoplasm

PM, plasma membrane; SF, stress fibers; FA, focal adhesions; agg, aggregates; n.d., not determined.

All chimeric proteins containing the amino-terminal 830 residues of supervillin were associated with actin filaments in the cytoskeleton and at plasma membranes, including sites at or near focal adhesion plaques. When overexpressed in the cytoplasm, these proteins formed bundles with actin filaments in spike-like cell surface extensions. When targeted to the nucleus, the supervillin amino terminus recruited actin into large coiled arrays. Thus, supervillin can bundle actin filaments *in vivo*, and this activity is potentiated by amino-terminal sequences. One possibility, which is supported by preliminary blot overlays of bacterial fusion proteins probed with <sup>125</sup>I-labeled F-actin (data not shown), is that the supervillin amino terminus contains two or more F-actin binding sites. Another possibility is that supervillin associations with itself or with other proteins contribute to the observed F-actin bundling activity. Direct or indirect interactions with other membrane skeleton proteins are consistent with the overlapping

### Supervillin Functional Domains

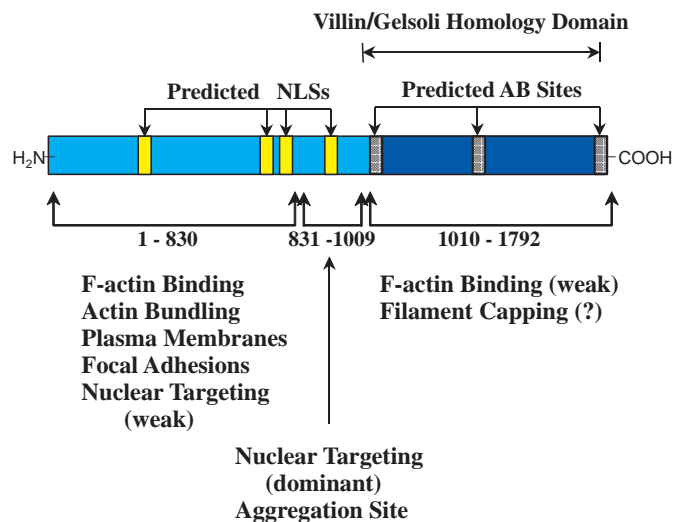


**Fig. 9.** Diagrammatic representation of bovine supervillin showing the conclusions drawn from this study. Predicted nuclear localization signals (NLSs) and actin binding (AB) sites are shown. Most of the currently identified functional sequences are in the supervillin-specific amino terminus rather than in the villin/gelsolin homology domain.

localizations of supervillin and the focal adhesion protein, vinculin, and by the disruption of focal adhesion plaque integrity upon overexpression of either full-length supervillin or the supervillin amino terminus. Also, supervillin is extracted from neutrophil plasma membranes as a detergent- and salt-resistant 26S complex that contains non-erythroid spectrin, as well as a number of other polypeptides (Pestonjamas et al., 1997).

All chimeric proteins containing amino acids 831 through 1009 were highly concentrated in the nucleus, where they often formed higher-order structures. In the case of EGFP-SV1-1009, these structures were large bundles of lamin-containing actin filaments, whereas amorphous aggregates were observed with chimeras that lacked the amino-terminal actin-bundling sequences. These results suggest that the fourth nuclear localization sequence at residues 931-935 (RPKRR), a canonical SV40-like nuclear localization signal (Chelsky et al., 1989), is the dominant signal for targeting supervillin to the nucleus. Our previous immunolocalization of supervillin to nuclei of subconfluent MDBK cells, and the exclusion of supervillin from nuclei in confluent cultures, suggest that nuclear targeting of supervillin is normally regulated by adhesion- or cell cycle-dependent processes (Pestonjamas et al., 1997). Our results also suggest that amino acids 831 through 1009 include a site that promotes aggregation of supervillin. Interestingly, this sequence contains two regions, amino acids 844-864 and 947-976, that are predicted by the COILS 2 program to be capable of forming short coiled-coils (Lupas, 1996).

Given the high conservation of the carboxy-terminal villin/gelsolin homology domain across species (Pope et al., 1998), it is likely that this region of supervillin is functionally important. However, only limited information about the intracellular functionality of this region resulted from our experiments. In agreement with the conclusion that segment 1 in both villin and gelsolin is required for actin filament severing activity (reviewed by Burtnick et al., 1997; Sun et al., 1994; Weeds and Maciver, 1993), we obtained no evidence for filament severing in cells that overexpress supervillin, which lacks significant similarity to segment 1 (Pestonjamas et al., 1997). The limited co-localization of Alexa<sup>TM</sup> 594-phalloidin and aggregates of EGFP-SV831-1792 or EGFP-SV831-1281 (Fig. 6) may be caused by low affinity binding of F-actin to the first predicted actin-binding site in supervillin (Fig. 9) (Pestonjamas et al., 1997), a sequence that is  $\geq 62\%$  identical to actin-binding sequences in segments 2 of villin and gelsolin (de Arruda et al., 1992). Indirect evidence for functionality of the supervillin carboxy terminus may be gleaned from the observation that chimeric proteins lacking amino acids 1010 to 1792 formed nuclear F-actin bundles that were much larger and thicker than cytoplasmic F-actin bundles generated by full-length supervillin. Thus, the supervillin carboxy terminus may control the lengths of actin filaments or filament bundles and/or contribute to the localization of the protein to the plasma membrane or cytoplasmic compartments. The former possibility is consistent with the report that *Dictyostelium* protovillin, a protein that is more similar to bovine supervillin than either sequence is to mammalian villins (Pestonjamas et al., 1997), is an actin filament capping protein that lacks filament severing and bundling activities (Hofmann et al., 1992, 1993). Because protovillin contains no significant

similarities to the amino-terminal actin-bundling sequences in supervillin, it is possible that the conserved carboxy-terminal sequences are involved in F-actin capping.

The absence of bundling activity associated with the supervillin carboxy terminus also is consistent with a previous mutational analysis of the chicken villin headpiece (Doering and Matsudaira, 1996). In this study, cysteine replacement mutagenesis of lysine-38 in bacterially-expressed headpiece reduced the binding of F-actin to  $\sim 30\%$  of that observed for the wild-type polypeptide. Because the corresponding residue in both the bovine and human supervillin headpiece is a leucine (amino acids 1754 and 1750, respectively), the prediction is that the supervillin headpiece should bind F-actin with a  $K_d$  of only  $\sim 21 \mu\text{M}$  (Pope et al., 1994). On the other hand, the dematin headpiece also contains a leucine at this position (Rana et al., 1993), but nevertheless binds to F-actin in vitro (Azim et al., 1995). Although it is possible that the supervillin carboxy terminus exhibits villin-like properties in some circumstances, e.g. after appropriate post-translational modification or by binding to an unknown allosteric regulator, it is clear that this region of supervillin does not, by itself, generate microspikes and elongated microvilli similar to those observed after overexpression or microinjection of villin (Franck et al., 1990; Friederich et al., 1989). Thus, the supervillin-specific sequences interspersed between the villin/gelsolin homology segments in the supervillin carboxy terminus (Pestonjamas et al., 1997) apparently confer on supervillin functionality and/or regulation distinct from that of villin. Based on the intriguing localizations reported here, we suggest that these functions may include recruitment of actin and other cytoskeletal proteins into specialized structures at the plasma membrane and/or in the nuclei of growing cells.

The authors thank L. Ohrn for preparation of media and reagents and D. Castellanos and M. Martineau for superb glassware washing. We also thank Dr Kathleen J. Green for a highly transfectable subclone of COS7-2 cells, and Drs Anne and Robert Goldman for antibodies against lamins A/C. J. D. Wulfschuh was supported by a National Institutes of Health (NIH) postdoctoral training fellowship (no. 5T32HD07312-12), I. E. Donina by a Summer Research Fellowship from a National Science Foundation REU Program grant (no. BIR-9423903), and R. K. Pope by an American Cancer Society postdoctoral fellowship (no. PF-4297). This research was supported by NIH grant GM33048 to E. J. Luna and also benefited from pilot grant support from the Worcester Foundation Board of Trustees. The contents of this publication are solely the responsibility of the authors and do not necessarily represent the official views of these funding agencies.

## REFERENCES

- Adams, C. L., Nelson, W. J. and Smith, S. J. (1996). Quantitative analysis of cadherin-catenin-actin reorganization during development of cell-cell adhesion. *J. Cell Biol.* **135**, 1899-1911.
- Arpin, M., Friederich, E., Algrain, M., Vernel, F. and Louvard, D. (1994). Functional differences between L- and T-plastin isoforms. *J. Cell Biol.* **127**, 1995-2008.
- Ayscough, K. (1998). Use of latrunculin-A, an actin monomer-binding drug. *Meth. Enzymol.* **298**, 18-25.
- Azim, A. C., Knoll, J. H., Beggs, A. H. and Chishti, A. H. (1995). Isoform cloning, actin binding, and chromosomal localization of human erythroid dematin, a member of the villin superfamily. *J. Biol. Chem.* **270**, 17407-17413.
- Bazari, W. L., Matsudaira, P., Wallek, M., Smeal, T., Jakes, R. and Ahmed,

- Y. (1988). Villin sequence and peptide map identify six homologous domains. *Proc. Nat. Acad. Sci. USA* **85**, 4986-4990.
- Ben-Ze'ev, A.** (1997). Cytoskeletal and adhesion proteins as tumor suppressors. *Curr. Opin. Cell Biol.* **9**, 99-108.
- Bershadsky, A. D., Gluck, U., Denisenko, O. N., Sklyarova, T. V., Spector, I. and Ben-Ze'ev, A.** (1995). The state of actin assembly regulates actin and vinculin expression by a feedback loop. *J. Cell Sci.* **108**, 1183-1193.
- Bretscher, A.** (1991). Microfilament structure and function in the cortical cytoskeleton. *Annu. Rev. Cell Biol.* **7**, 337-374.
- Bretscher, A.** (1999). Regulation of cortical structure by the ezrin-radixin-moesin protein family. *Curr. Opin. Cell Biol.* **11**, 109-116.
- Burridge, K. and Chrzanoska-Wodnicka, M.** (1996). Focal adhesions, contractility, and signaling. *Annu. Rev. Cell Dev. Biol.* **12**, 463-518.
- Burtnick, L. D., Koepf, E. K., Grimes, J., Jones, E. Y., Stuart, D. I., McLaughlin, P. J. and Robinson, R. C.** (1997). The crystal structure of plasma gelsolin: implications for actin severing, capping, and nucleation. *Cell* **90**, 661-670.
- Chelsky, D., Ralph, R. and Jonak, G.** (1989). Sequence requirements for synthetic peptide-mediated translocation to the nucleus. *Mol. Cell Biol.* **9**, 2487-2492.
- Coluccio, L. M. and Tilney, L. G.** (1984). Phalloidin enhances actin assembly by preventing monomer dissociation. *J. Cell Biol.* **99**, 529-535.
- Cormack, B. P., Valdivia, R. H. and Falkow, S.** (1996). FACS-optimized mutants of the green fluorescent protein (GFP). *Gene* **173**, 33-38.
- Craig, S. W. and Johnson, R. P.** (1996). Assembly of focal adhesions: progress, paradigms, and portents. *Curr. Opin. Cell Biol.* **8**, 74-85.
- de Arruda, M. V., Bazari, H., Wallek, M. and Matsudaira, P.** (1992). An actin footprint on villin. Single site substitutions in a cluster of basic residues inhibit the actin severing but not capping activity of villin. *J. Biol. Chem.* **267**, 13079-13085.
- Dedhar, S. and Hannigan, G. E.** (1996). Integrin cytoplasmic interactions and bidirectional transmembrane signalling. *Curr. Opin. Cell Biol.* **8**, 657-669.
- Doering, D. S. and Matsudaira, P.** (1996). Cysteine scanning mutagenesis at 40 of 76 positions in villin headpiece maps the F-actin binding site and structural features of the domain. *Biochemistry* **35**, 12677-12685.
- Fath, K. R. and Burgess, D. R.** (1995). Not actin alone. *Curr. Biol.* **5**, 591-593.
- Finidori, J., Friederich, E., Kwiatkowski, D. J. and Louvard, D.** (1992). In vivo analysis of functional domains from villin and gelsolin. *J. Cell Biol.* **116**, 1145-1155.
- Franck, Z., Footer, M. and Bretscher, A.** (1990). Microinjection of villin into cultured cells induces rapid and long-lasting changes in cell morphology but does not inhibit cytokinesis, cell motility, or membrane ruffling. *J. Cell Biol.* **111**, 2475-2485.
- Friederich, E., Huet, C., Arpin, M. and Louvard, D.** (1989). Villin induces microvilli growth and actin redistribution in transfected fibroblasts. *Cell* **59**, 461-475.
- Furukawa, R. and Fechheimer, M.** (1997). The structure, function, and assembly of actin filament bundles. *Int. Rev. Cytol.* **175**, 29-90.
- Gant, T. M. and Wilson, K. L.** (1997). Nuclear assembly. *Annu. Rev. Cell Dev. Biol.* **13**, 669-695.
- Glenney, J. R. Jr, Geisler, N., Kaulfus, P. and Weber, K.** (1981). Demonstration of at least two different actin-binding sites in villin, a calcium-regulated modulator of F-actin organization. *J. Biol. Chem.* **256**, 8156-8161.
- Glück, U., Kwiatkowski, D. J. and Ben-Ze'ev, A.** (1993). Suppression of tumorigenicity in simian virus 40-transformed 3T3 cells transfected with alpha-actinin cDNA. *Proc. Nat. Acad. Sci. USA* **90**, 383-387.
- Glück, U. and Ben-Ze'ev, A.** (1994). Modulation of alpha-actinin levels affects cell motility and confers tumorigenicity on 3T3 cells. *J. Cell Sci.* **107**, 1773-1782.
- Gumbiner, B. M.** (1996). Cell adhesion: The molecular basis of tissue architecture and morphogenesis. *Cell* **84**, 345-357.
- Heintzelman, M. B. and Mooseker, M. S.** (1992). Assembly of the intestinal brush border cytoskeleton. *Curr. Topics Dev. Biol.* **26**, 93-122.
- Hofmann, A., Eichinger, L., Andre, E., Rieger, D. and Schleicher, M.** (1992). Cap100, a novel phosphatidylinositol 4,5-bisphosphate-regulated protein that caps actin filaments but does not nucleate actin assembly. *Cell Motil. Cytoskel.* **23**, 133-144.
- Hofmann, A., Noegel, A. A., Bomblies, L., Lottspeich, F. and Schleicher, M.** (1993). The 100 kDa F-actin capping protein of Dictyostelium amoebae is a villin prototype ('protovillin'). *FEBS Lett.* **328**, 71-76.
- Ikeda, K., Kaub, P. A., Asada, H., Uyemura, K., Toya, S. and Shirao, T.** (1996). Stabilization of adhesion plaques by the expression of drebrin A in fibroblasts. *Brain Res. Dev. Brain Res.* **91**, 227-236.
- Ishikawa, R., Hayashi, K., Shirao, T., Xue, Y., Takagi, T., Sasaki, Y. and Kohama, K.** (1994). Drebrin, a development-associated brain protein from rat embryo, causes the dissociation of tropomyosin from actin filaments. *J. Biol. Chem.* **269**, 29928-29933.
- Kartenbeck, J., Schmelz, M., Franke, W. W. and Geiger, B.** (1991). Endocytosis of junctional cadherins in bovine kidney epithelial (MDBK) cells cultured in low Ca<sup>2+</sup> ion medium. *J. Cell Biol.* **113**, 881-892.
- Knudsen, K. A., Soler, A. P., Johnson, K. R. and Wheelock, M. J.** (1995). Interaction of alpha-actinin with the cadherin/catenin cell-cell adhesion complex via alpha-catenin. *J. Cell Biol.* **130**, 67-77.
- Kowalczyk, A. P., Bornslaeger, E. A., Borgwardt, J. E., Palka, H. L., Dhaliwal, A. S., Corcoran, C. M., Denning, M. F. and Green, K. J.** (1997). The amino-terminal domain of desmoplakin binds to plakoglobin and clusters desmosomal cadherin-plakoglobin complexes. *J. Cell Biol.* **139**, 773-784.
- Lelèvre, S. A. and Bissell, M. J.** (1998). Communication between the cell membrane and the nucleus: Role of protein compartmentalization. *J. Cell. Biochem. Suppl.* **30/31**, 250-263.
- Louvard, D., Kedinger, M. and Hauri, H. P.** (1992). The differentiating intestinal epithelial cell: establishment and maintenance of functions through interactions between cellular structures. *Annu. Rev. Cell Biol.* **8**, 157-195.
- Luna, E. J.** (1998). F-actin blot overlays. *Meth. Enzymol.* **298**, 32-42.
- Luna, E. J. and Hitt, A. L.** (1992). Cytoskeleton-plasma membrane interactions. *Science* **258**, 955-964.
- Luna, E. J., Pestonjamas, K. N., Cheney, R. E., Strassel, C. P., Lu, T. H., Chia, C. P., Hitt, A. L., Fechheimer, M., Furthmayr, H. and Mooseker, M. S.** (1997). Actin-binding membrane proteins identified by F-actin blot overlays. *Soc. Gen. Physiol. Ser.* **52**, 3-18.
- Lupas, A.** (1996). Coiled coils: new structures and new functions. *Trends Biochem. Sci.* **21**, 375-382.
- Melan, M. A. and Sluder, G.** (1992). Redistribution and differential extraction of soluble proteins in permeabilized cultured cells. Implications for immunofluorescence microscopy. *J. Cell Sci.* **101**, 731-743.
- Moir, R. D., Spann, T. P. and Goldman, R. D.** (1995). The dynamic properties and possible functions of nuclear lamins. *Int. Rev. Cytol.* **141**-182.
- Pavalko, F. M. and Burridge, K.** (1991). Disruption of the actin cytoskeleton after microinjection of proteolytic fragments of alpha-actinin. *J. Cell Biol.* **114**, 481-491.
- Pavalko, F. M., Schneider, G., Burridge, K. and Lim, S.-S.** (1995). Immunodetection of alpha-actinin in focal adhesions is limited by antibody inaccessibility. *Exp. Cell Res.* **217**, 534-540.
- Pestonjamas, K., Amieva, M. R., Strassel, C. P., Nauseef, W. M., Furthmayr, H. and Luna, E. J.** (1995). Moesin, ezrin, and p205 are actin-binding proteins associated with neutrophil plasma membranes. *Mol. Biol. Cell* **6**, 247-259.
- Pestonjamas, K. N., Pope, R. K., Wulfkuhle, J. D. and Luna, E. J.** (1997). Supervillin (p205): A novel membrane-associated, F-actin-binding protein in the villin/gelsolin superfamily. *J. Cell Biol.* **139**, 1255-1269.
- Peters, R.** (1986). Fluorescence microphotolysis to measure nucleocytoplasmic transport and intracellular mobility. *Biochim. Biophys. Acta* **864**, 305-359.
- Pope, B., Way, M., Matsudaira, P. T. and Weeds, A.** (1994). Characterisation of the F-actin binding domains of villin: classification of F-actin binding proteins into two groups according to their binding sites on actin. *FEBS Lett.* **338**, 58-62.
- Pope, R. K., Pestonjamas, K. N., Smith, K. P., Wulfkuhle, J. D., Strassel, C. P., Lawrence, J. B. and Luna, E. J.** (1998). Cloning, characterization, and chromosomal localization of human supervillin (SVIL). *Genomics* **52**, 342-351.
- Prasher, D. C., Eckenrode, V. K., Ward, W. W., Prendergast, F. G. and Cormier, M. J.** (1992). Primary structure of the Aequorea victoria green-fluorescent protein. *Gene* **111**, 229-233.
- Rana, A. P., Ruff, P., Maalouf, G. J., Speicher, D. W. and Chishti, A. H.** (1993). Cloning of human erythroid dematin reveals another member of the villin family. *Proc. Nat. Acad. Sci. USA* **90**, 6651-6655.
- Robinson, D. N. and Cooley, L.** (1997). Genetic analysis of the actin cytoskeleton in the *Drosophila* ovary. *Annu. Rev. Cell Dev. Biol.* **13**, 147-170.
- Ruoslahti, E. and Reed, J. C.** (1994). Anchorage dependence, integrins, and apoptosis. *Cell* **77**, 477-478.
- Sasaki, Y., Hayashi, K., Shirao, T., Ishikawa, R. and Kohama, K.** (1996). Inhibition by drebrin of the actin-bundling activity of brain fascin, a protein localized in filopodia of growth cones. *J. Neurochem.* **66**, 980-988.

- Schafer, D. A. and Cooper, J. A.** (1995). Control of actin assembly at filament ends. *Annu. Rev. Cell Dev. Biol.* **11**, 497-518.
- Schultheiss, T., Choi, J., Lin, Z. X., DiLullo, C., Cohen-Gould, L., Fischman, D. and Holtzer, H.** (1992). A sarcomeric  $\alpha$ -actinin truncated at the carboxyl end induces the breakdown of stress fibers in PtK2 cells and the formation of nemaline-like bodies and breakdown of myofibrils in myotubes. *Proc. Nat. Acad. Sci. USA* **89**, 9282-9286.
- Shirao, T., Kojima, N. and Obata, K.** (1992). Cloning of drebrin A and induction of neurite-like processes in drebrin-transfected cells [published erratum appears in *Neuroreport* 1992 Mar;3(3):following 285]. *Neuroreport* **3**, 109-112.
- Shirao, T.** (1995). The roles of microfilament-associated proteins, drebrins, in brain morphogenesis: a review. *J. Biochem (Tokyo)* **117**, 231-236.
- Shutt, D. C., Wessels, D., Wagenknecht, K., Chandrasekhar, A., Hitt, A. L., Luna, E. J. and Soll, D. R.** (1995). Ponticulin plays a role in the positional stabilization of pseudopods. *J. Cell Biol.* **131**, 1495-1506.
- Sun, H. Q., Wooten, D. C., Janmey, P. A. and Yin, H. L.** (1994). The actin side-binding domain of gelsolin also caps actin filaments. Implications for actin filament severing. *J. Biol. Chem.* **269**, 9473-9479.
- Taylor, K. and Taylor, D.** (1994). Formation of two-dimensional complexes of F-actin and crosslinking proteins on lipid monolayers: Demonstration of unipolar alpha-actinin-F-actin crosslinking. *Biophys. J.* **67**, 1976-1983.
- Tilney, L. G., Tilney, M. S. and DeRosier, D. J.** (1992). Actin filaments, stereocilia, and hair cells: How cells count and measure. *Annu. Rev. Cell Biol.* **8**, 257-274.
- Tilney, L. G., Tilney, M. S. and Guild, G. M.** (1995). F actin bundles in *Drosophila* bristles. I. Two filament cross-links are involved in bundling. *J. Cell Biol.* **130**, 629-638.
- Vaheri, A., Carpen, O., Heiska, L., Helander, T. S., Jaaskelainen, J., Majander-Nordenswan, P., Sainio, M., Timonen, T. and Turunen, O.** (1997). The ezrin protein family: membrane-cytoskeleton interactions and disease associations. *Curr. Opin. Cell Biol.* **9**, 659-666.
- Way, M., Gooch, J., Pope, B. and Weeds, A. G.** (1989). Expression of human plasma gelsolin in *Escherichia coli* and dissection of actin binding sites by segmental deletion mutagenesis. *J. Cell Biol.* **109**, 593-605.
- Weeds, A. and Maciver, S.** (1993). F-actin capping proteins. *Curr. Opin. Cell Biol.* **5**, 63-69.
- Weisberg, E., Sattler, M., Ewaniuk, D. S. and Salgia, R.** (1997). Role of focal adhesion proteins in signal transduction and oncogenesis. *Crit. Rev. Oncog.* **8**, 343-358.
- Wulfschuh, J. D., Petersen, N. S. and Otto, J. J.** (1998). Changes in the F-actin cytoskeleton during neurosensory bristle development in *Drosophila*: the role of singed and forked proteins. *Cell Motil. Cytoskel.* **40**, 119-132.
- Yamashiro, S., Yamakita, Y., Ono, S. and Matsumura, F.** (1998). Fascin, an actin-bundling protein, induces membrane protrusions and increases cell motility of epithelial cells. *Mol. Biol. Cell* **9**, 993-1006.